URSI - RCRS 2022, IIT (Indore), India, 1 - 4 December, 2022

Results from Solar Coronal Sounding Experiments Conducted by Indian Mars Orbiter Mission (MOM) during Mars-Solar Conjunctions

Richa N. Jain*[1], R. K. Choudhary[1], and Anil Bhardwaj[2], Umang Parikh[3], Bijoy K. Dai[3], and Roopa M.V.[3]

[1]Space physics Laboratory, VSSC, Trivandrum, India
[2]Physical Research Laboratory, Ahmedabad, India
[3]ISRO Telemetry Tracking and Command Network, Bengaluru, India

1. Abstract

Indian Mars Orbiter Mission is India's first interplanetary mission, which was inserted into Martian orbit in 2014. We analyzed the downlink S-band radio signals sent from the spacecraft and received at Indian Deep Space Network, Bangalore during the May-June 2015, and September-October 2021 solar conjunction events. The experiment geometry helped us to probe the coronal region at heliocentric distances between 4 and 20 $R_\odot$ (1 $R_\odot$ = 676,900 Km) when the solar activity was at the post-maximum phase of the solar cycle 24, and ascending phase of the Solar cycle 25. Frequency residuals obtained from signals were spectrally analyzed to study coronal plasma turbulence. It is observed that the changes in turbulence regime with respect to heliocentric distances are well reflected in spectral index values from frequency fluctuation spectrum. At a lower heliocentric distance (<10 $R_\odot$), the spectrum has flattened with spectral index $\alpha_f \sim 0.3 - 0.5$, which corresponds to the energy source input regime. For larger heliocentric distances (> 10$R_\odot$), the curve steepens with spectral index $\alpha_f \sim 0.7 - 0.8$, a value close to 2/3, that is indicative of inertial regimes of developed Kolmogorov-type turbulence where energy is transported through cascading. This helped us to understand the processes in the transition region where solar wind accelerates from subalfvenic to superalfvenic speeds. This study proposes interesting insights into how solar wind properties near the coronal regions can be investigated using the radio-sounding method, which is an effective method to study complex coronal physics.

2. Introduction

Solar Conjunction is the period when a planet is on the opposite side of the Sun than the Earth. During this time, the radio signals transmitted by spacecraft orbiting planets travel closer to the solar corona region and are then received at the ground station. Corona is the outer atmosphere of the Sun which is dominated by the complex interplay of magnetic fields, high temperatures, and turbulent plasma. These conditions make the in-situ studies of this region quite challenging. In this context, the next most reliable and widely used technique to probe this region is through remote sensing via the radio signals transmitted by the spacecraft. As the solar corona is an ionized plasma, dispersive effects (frequency fluctuations, doppler) gets registered in the parameters of the received electromagnetic wave. It is known that the dispersion relation of plasma is a function of electron density of the medium and frequency of incident EM wave. Radio coronal sounding experiments utilize this principle to retrieve the properties of plasma medium from observed Doppler shifts and fluctuations in the received signal.

The high temperature in the Corona creates a pressure gradient, which propels the ionized charged particles outward from the corona and towards the interplanetary medium. This ubiquitous flow of charged particles is the solar wind [1]. Solar wind particles travel across the interplanetary medium, shapes the magnetosphere of planets, and ultimately affect the space weather phenomenon near-earth environment. The Coronal transition region [2] is primarily the region where the solar wind gets energized and gains momentum to attain the velocity recorded at the L1 point of the Earth by the satellites. Hence, further insights into the coronal dynamics and acceleration of the solar wind, especially during various periods of activities at different solar cycles hold immense importance in augmenting our understanding of space weather phenomena.

As proposed by Parker [1], the main factor which causes the acceleration of the solar wind is the high temperature of Corona. However, this raises a pertinent question: what is the mechanism behind the heating of Solar Corona? Several explanations are presented [2,3], with the prominent one that attributes the coronal heating to the phenomenon of turbulence and dissipation of energy contained in the magnetohydrodynamic (MHD) waves, that travel across the low-beta plasma region of the Coronal region. Mainly there are two types of wind based on their difference in speeds and density: Fast Solar wind and Slow Solar wind. Fast solar winds originate in coronal holes, the darker regions at higher heliolatitudes with open field lines [4]. Slow solar winds, on the other hand, originate above the active regions in streamer belts, which are mostly found at equatorial heliolatitudes [5].

Turbulence in the coronal plasma is an omnipresent feature at all heliolatitudes and heliocentric distances and causes fluctuation in the coronal medium properties such as electron density and magnetic fields in the region [6,7,8]. Acceleration of outward going charged particles that constitute the solar wind is caused by the cascading of the energy of Alfven waves into magnetosonic waves, which dissipate and heat the Corona [6] and creates a thermal pressure gradient that accelerates the solar wind such that it flows from being subsonic to supersonic and super-Alfven beyond a certain distance termed Alfvenic surface and continues in the interplanetary medium [9]. Alfvenic surface defines the boundary between the corona and solar wind where solar wind velocity exceeds the background Alfven wave speed [9].

Though the solar wind properties are explained by several models [10,11] including previous observations using radio-sounding experiments from various spacecraft such as HELIOS in 1975–1976 [12], Ulysses in 1991 [13], Galileo in 1994–2002 [14], MESSENGER in 2009 [12], Rosetta and Mars Express in 2010/2011 [15], and Indian Mars Orbiter Mission in 2015 [16], further studies at various heliocentric distances, at different phases of solar cycles, probing different coronal region are needed in order to gain a better understanding into the phenomena of coronal heating, solar wind acceleration and dynamics across the alfvenic surface.

In this present work, we used the S-band radio signals transmitted from the Indian Mars Orbiter Mission (MOM) during the 2015 Mars-Solar conjunction events which correspond to the near-maximum declining phase of solar cycle 24. Another radio-sounding experiment was conducted during the 2021 conjunction event, which corresponds to the ascending phase of solar cycle 25 when the solar activity started increasing after minima in 2019.

The MOM spacecraft, India's first mission to Mars, was launched on 2013 November 5, and inserted into the Martian orbit on 2014 September 24, after 299 days of travel. It successfully completed the planned mission lifetime of 6 months, went on to surpass this by a factor of 10 (∼7 years), and now is in the extended mission phase. The MOM spacecraft has a highly elliptical orbit, with an apoapsis of ∼71 000 km and periapsis varying from ∼260 to ∼550 km. For communicating with the Earth, the MOM spacecraft uses an offset parabolic disc reflector high-gain antenna with a diameter of 2.2 m. The operating frequency of the antenna during the operation was 2292.96 MHz. The consumed input DC power of the antenna system was 440 W. 2015 conjunction experiment was conducted the period between 2015 May 28 and June 26. S-band radio signals were sent from the MOM spacecraft and received at the Indian Deep Space Network (IDSN), Byallalu, Bangalore using an on-site 32-m antenna. During this period, the MOM to D32 station distance was∼379.78 million km. The average received signal power was about –134 dBm. [16].

Due to the relative orbital geometry of MOM and D32 station at Bangalore we were able to probe the heliocentric distances as close as 4 −20 $R_{\odot}$. The methodology to process frequency fluctuation data, and intriguing results along with the interpretation from the solar wind turbulence spectrum are mentioned in the subsequent sections.

3. Data Processing and Observations

3.1 May-June 2015 Conjunction

The experiments were conducted using radio signals (S-band downlink frequency 2.29 GHz) sent by MOM spacecraft, during the 2015 May-June conjunction, when Sun was between Earth and Mars along the line in the same ecliptic plane as depicted in Fig 1(a). The signals were recorded at IDSN, Bangalore. This experiment was performed in closed-loop format and the sampling frequency was 1 Hz.

The conjunction happened in 2015, which was the near-maximum phase of solar cycle 24 when the solar activity has just started declining after the maxima of 2014. Solar cycle 24 was a peculiar cycle in the terms of its overall diminished sunspots number. Fig 1(b) shows the image of the corona on 2015 June 6 as recorded by AIA/SDO depicting the active region on the coronal disc. The occultation experiment geometry was such that the solar offset distances (where the radio ray path reaches its closest point to the Sun), were between 4 to 20 $R_{\odot}$ and covered low-equatorial heliolatitudes (5° to 39°).

The received signals were processed to find the observed Doppler shift using the standard technique as adopted in radio occultation experiments [16,17]. The geometrical expected Doppler was calculated using relative ephemeris data (position and velocity) provided by the MOM mission team. Their difference gives the values of Doppler frequency residuals. In order to take into account errors arising from systematic sources such as oscillator drifts, imperfections in trajectory, and the effect of terrestrial ionosphere and atmosphere, a linear regression was estimated and subtracted from frequency residuals. This gave fluctuations in the residual values around zero mean value. Using the Fast Fourier Transform (FFT) algorithm these values were spectrally analyzed to give the frequency fluctuation spectrum.

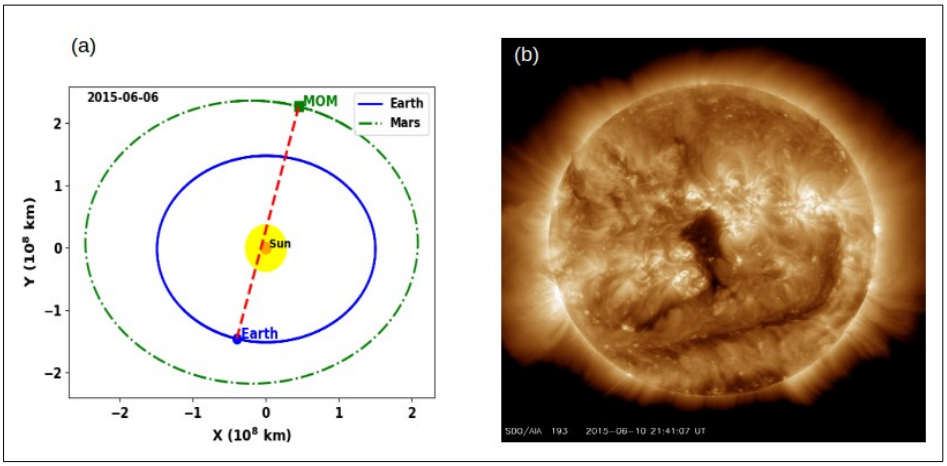

Figure 1. (a) Schematic of positions of Earth and MOM spacecraft relative to Sun on 2015 June 6, on XY plane as seen from north in ECLIPJ2000 reference frame. (b) Photograph of Coronal disc on 2015 June 10 as recorded by SDO/AIA instrument in 193 Å.

Frequency fluctuation spectra were approximated by fitting a straight line (in log-log plot), in the frequency range v_{lo} and v_{up}. The lower-frequency cutoff $v_{lo} = 10^{-3}$ Hz is the length of the processed interval and the upper cutoff $v_{up} = 0.05$ Hz is one-tenth of the Nyquist frequency (considering that sample rate is 1Hz, and beyond nyquist frequency systems noise begins to dominate the signal.) The slope then can be estimated directly by the linear fit on the log-log plot. Fig 2 shows the temporal spectra of frequency fluctuations during two different experiment days. The slope (red straight line) denotes the value of spectral index α_f .

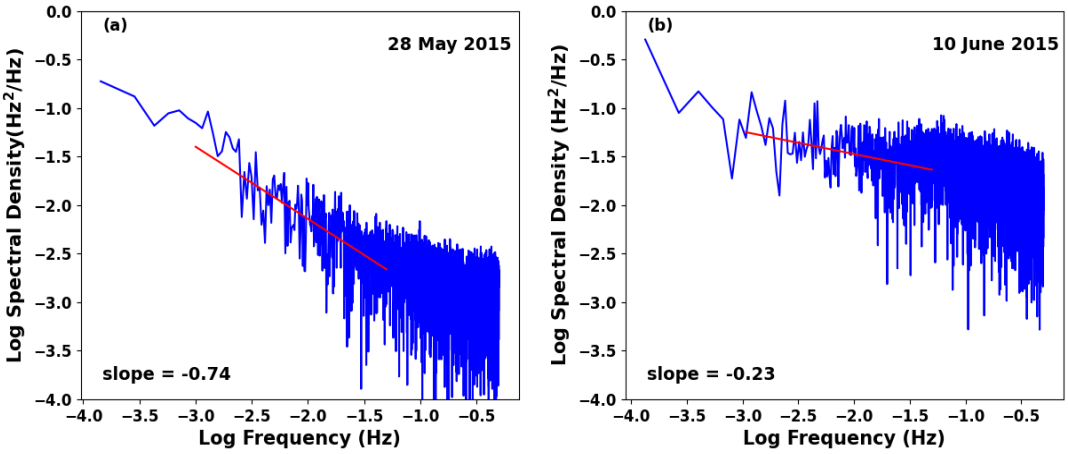

Figure 2. (a) Frequency fluctuation spectrum of the MOM downlink signal on 2015 May 28 when the heliocentric distance of the proximate ray path was r = 18.17 $R_\odot$, and the spectral index = slope = $\alpha_f = -0.74$. (b) Frequency fluctuation spectrum on 2015 June 10 when r = 5.33 $R_\odot$, and the spectral index = slope = $\alpha_f = -0.23$, Flatter spectra [16].

This frequency fluctuation spectrum is related to the turbulence spectrum of the plasma density based on the isotropic quasi-static turbulence model [14,16,18], which is discussed in the subsequent section. According to it, the slope of the frequency fluctuation turbulence spectrum (in log-log format) corresponds to the spectral power index value α, which relates to the plasma density turbulence regimes in the coronal region. As can be seen in fig 2(a) on 2015 May 28, the proximate distance of the radio ray path was 18.17 Rs and the slope of the turbulence spectrum was 0.74. According to the theory of Kolmogorov turbulence, this is an inertial turbulence regime. Here, it is assumed that the energy cascading process has been set up. In fig 2(b), on 2015 June 6, when the proximate ray path distance was 5.33 Rs the slope values were steeper -0.23.

These lower values of spectral index denote the underdeveloped turbulence and it usually corresponds to the source regime, that when energy is being given in the system.

Table 1 denotes the slope α_f for different experiment days, which corresponds to the different heliocentric distances and heliolatitudes of the solar proximate ray path point. It can be observed that for distances closer to the solar surface i.e. at lower heliocentric distances (2-10 $R_\odot$), the spectrum is generally flatter with a slope of $\alpha_f \sim 0.2\text{-}0.5$. At the larger heliocentric distances (>10 $R_\odot$) of the proximate ray path point, the spectra become steeper with the slope in ranges of $\alpha_f \sim 0.6 - 0.8$ and gave the appearance of developed Kolomogrov type turbulence. These observations based on the change in the slope of the temporal frequency fluctuation spectrum denote the changes in the regime of the plasma density turbulence in the solar corona with the changing heliocentric distances.

Table 1. Results of radio-sounding measurements conducted during 2015 Conjunction.

Date	Solar Offset($R_\odot$)	Heliolat (deg)	Spectral Index
28/05/15	18.17	5.59	0.741
02/06/15	13.19	8.49	0.717
04/06/15	11.24	10.37	0.649
06/06/15	9.22	13.01	0.427
08/06/15	7.23	17.28	0.327
10/06/15	5.33	24.59	0.241
12/06/15	3.6	39.33	0.288
18/06/15	4.28	35.32	0.339
20/06/15	6.28	24.39	0.272

This transition in plasma turbulence regime is consistent with what was observed in similar previous studies conducted on the other dispersive parameters such as phase scintillation spectra, spectra in amplitude fluctuations and magnetic field power spectra at similar heliocentric distances. Interestingly, these results on observation of turbulence transition regime have also been supported by the first time the in-situ measurement conducted by the Parker probe during its 2021 flyby [19].

3.2 September - October 2021 Conjunction

Due to the orbital revolution period of Mars which is twice as that of Earth, the relative Mars-Earth-Solar conjunction occurs approximately every two years. A special solar radio sounding experiment was planned during September-October period using DeltaDOR experimental setup. Due to some technical issues, however the data collection duration has been limited. The experiment was performed in the open loop and data was recorded in the RDEF format. The solar offset (proximate point of ray path from the solar surface) of the radio signal ray is 5-8 $R_\odot$ and mostly spanning low-equatorial heliolatitudes. The frequency residual values have been extracted from the data. The observed features are in the line of the results as for the previous measurements during the similar solar activity.

4. Isotropic Quasi-static Turbulence Model

This is a well-studied model for the “frozen-in” solar wind turbulence [12,18,20], which is based on the assumption that spatial electron density inhomogeneities in the Coronal plasma medium have a quasi-static isotropic 3D spectrum, turbulence in the plasma medium produces the fluctuations in the density. The dispersion relation of the plasma medium is the function of the electron density of the plasma and the frequency of incident electromagnetic waves. These in-homogeneity patterns move with the solar wind plasma across the sounding radio ray path. Thus, these turbulence-produced density fluctuations get registered as the fluctuations in the phase of the electromagnetic radio ray (corresponding to the doppler shift in the recorded frequency) propagating through that medium.

The observed statistical radio occultation signal parameter, here frequency fluctuation, is related to the spatial turbulence density spectrum as per the theoretical Armand-Efimov [14,18] isotropic turbulence model. This model is based on the theory

of radio wave propagation in a turbulent medium. The spectral power density can be represented by the isotropic power-law spectrum represented by the following expression [14] :

$$\Phi_N(q,R) = C^2(R)\left(q^2 + q_o^2\right)^{(-p/2)} \exp\left(-q^2/q_m^2\right)$$

where q is spatial wavenumber, R is the radial distance of solar proximate point, p is the spectral index of the spatial turbulence power spectrum. The q_o, q_m are the inner and outer scale of turbulence power spectrum. C(R) is the structure function characterizing the intensity of the electron density fluctuations in the turbulent medium.

Consider the radio waves of wavelength λ passing through a minimum solar offset distance R. Armand-Efimov model takes in account that near Sun, the spatial fluctuations are "frozen-in" and are convected outward at a velocity V of the solar wind. Then using the principles of geometric optics approximation and propagation of EM waves [ref], the temporal spectrum of frequency fluctuations, where spectral density is denoted by $G_f(\nu, R)$ in a radio - occulted signal is found to be :

$$G_f(\nu,R) = (1/2\pi)\, F_p(R)\, V\, \nu_0^{\alpha}\, \nu^2 \left(\nu^2 + \nu_0^2\right)^{(-(\alpha+2)/2)} \exp\left(-\nu^2/\nu_m^2\right)$$

with,

$$F_p(R) = 2(p-3) r_e^2 \lambda^2 < \sigma_N^2(R) > L$$

where F_p is function containing electron density fluctuation sigma, ν is the fluctuation frequency ($\nu = qV/2\pi$), V is the convective velocity of the solar wind plasma and r_e is the classic electron radius. The expression relates the spectral index of frequency fluctuation spectrum alpha to the electron density turbulence spatial turbulence spectrum p as $\alpha_f = p-3$ for 3D turbulence [16].

The spectral index of $\alpha_f \sim 0.6$-0.7 of the frequency fluctuations lies close to the spectral index of fully developed 3D Kolmogorov electron density turbulence spectrum p = 11/3 (as $\alpha_f = p-3$) [20]. This denotes the inertial range of the developed turbulence regime where energy is transported through cascading. Lower $\alpha_f \sim 0.2$-0.5 values denotes the energy source regime where turbulence is still underdeveloped [16,18].

5. Discussions

Our results (Table 1) denotes that the plasma turbulence at larger heliocentric $R > 10R_\odot$ is developed (spectral index $\alpha_f \sim 0.6 - 0.8$) in comparison to smaller heliocentric distances $R < 10R_\odot$,where the turbulence is weak with (spectral index value $\alpha_f \sim 0.2 - 0.5$). The above results are interpreted according to the solar wind turbulence theories [14,18,21] , which consider that solar wind turbulence is driven by the interaction of Magnetohydrodynamic (MHD) waves with the solar plasma particles. This turbulence sets up the energy transfer in the coronal region, heats the coronal medium and led to the supersonic acceleration of the solar wind plasma propagating in the interplanetary medium.

Low-frequency Alfven waves emerge from the base of the solar corona, they propagate outwards, and carry huge amounts of energy, which is the source of the turbulence [7]. Near the Corona ($<10\ R_\odot$), the solar magnetic field is strong and so the speed of the Alfven waves is higher than that of the sound waves. This is also the region where energy (in the form of Alfven waves) is injected into the region. This leads to underdeveloped turbulence and the power spectrum is a flatter slope with $\alpha_f \sim 0.2 - 0.5$ for the closer heliocentric distance ($<10\ R_\odot$). These power spectra are non-cascading, i.e. turbulence energy flux to the higher frequencies is absent and hence frequency spectrum with the flatter plateaus are observed.

With the increasing heliocentric distances, the magnetic field and also solar densities decrease radially. Further, the ratio of sound speed to the Alfven wave speed also increases. As a result, through an enhanced non-linear process, parametric decay instability develops in this low-beta plasma region. A forward propagating Alfven wave decomposes into backward propagating secondary Alfven wave and forward propagating ion-acoustic (magnetosonic) waves. Magnetosonic waves are plasma waves that propagate randomly and create the density and magnetic field fluctuations in the plasma, thereby setting up the turbulence in the medium. [21]. This turbulence activates the cascading process, i.e. the energy is being transferred from larger wavenumbers (i.e. lower frequencies) to smaller wavenumbers (higher frequencies), and this is reflected in the steeper power spectrum with $\alpha_f \sim 0.6 - 0.7$ denoting inertial regime of developed Kolmogorov type turbulence (p=11/3, $\alpha_f = 2/3$), which was observed in the turbulence spectrum beyond 10Rs. These magnetosonic waves then dissipate rapidly in the coronal medium, this heats up the coronal medium and thus accelerates the solar wind particles to the supersonic level.

Beyond 20 Rs, turbulence is fully developed and solar wind continues in the interplanetary medium as supersonic and superalfvenic flow.

This change in turbulence regime is well reflected in the spectral index values from our study of the MOM data as can be seen in Figure 3(a). We can notice that the transition in the turbulence regime takes place between the 10-20 $R_\odot$ and if it is corresponded with the theory of the solar wind acceleration by coronal heating due to MHD waves turbulence, then this gives a very strong indication that the around this region solar wind speed exceeds the background plasma Aflvenic speed. This is indicative of the locus of the Aflvenic surface which marks the boundary between Solar Corona and Solar wind. Incidentally, this result is also supported by the first direct observation of the solar corona from the parker probe 2021 flyby, when it measured the transition in turbulence regime and located the Aflvenic surface to be around 18 $R_\odot$, published independently in the very recent study [19]. The comparative study of turbulence spectrum obtained from these radio science experiments conducted at various phases of solar cycles can be used to study the effects of coronal features, whose prevalence varies at different phases of solar cycles, on the location of the Alfvenic surface.

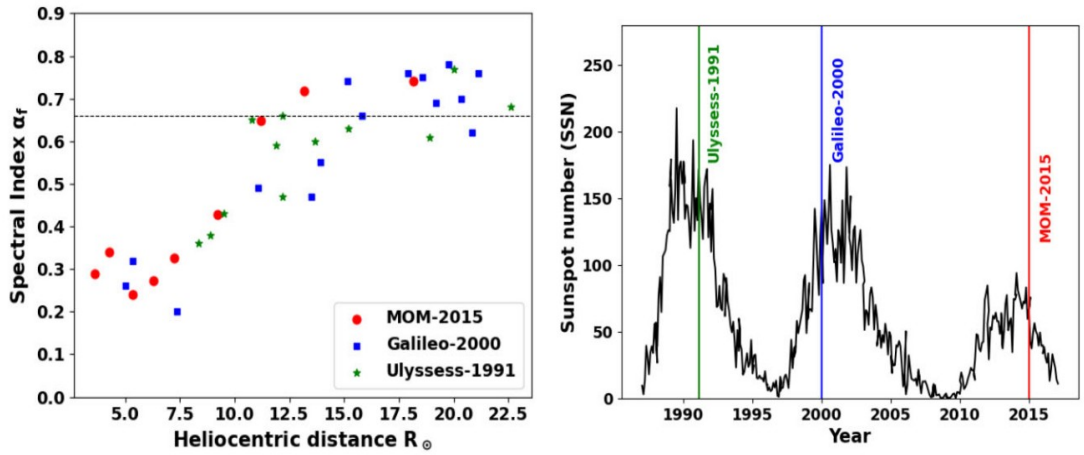

Figure 3. (a) Spectral index α_f of frequency fluctuation spectrum of the coronal radio sounding experiments conducted by MOM, Galileo and Ulyssess. (b) Average sunspot number over years 1987-2016, vertical lines mark the period when radio experiments where conducted by spacecrafts. [16].

We also compared values of the spectral index with respect to heliocentric distances as observed by previous studies which were conducted by spacecraft during the different solar cycles around the similar near maxima phase. The data for Ulysses experiment in 1991 and Galileo in 2000 corresponds to near maxima of solar cycle 22 and cycle 23 respectively, refer to Figure 3. It can be observed that the spectral index value $\alpha_f \sim 0.6 - 0.7$ which indicates the transition from the source regime to the Kolmogorov regime, happens at a lower heliocentric distance for MOM observations in the period compared to the previous solar cycle. This could be interpreted as one of the implications of the lack of active source regions on the solar corona. Hence, these observations also provide an interesting insight into the peculiar feeble maximum of the solar cycle 24 and its impact on the coronal dynamics conditions near Sun. [16]

6. Conclusions

Utilizing the solar conjunction event, when the Earth and Mars are on the opposite sides of the Sun, we studied the solar coronal dynamics and the turbulence in the solar coronal region as close as heliocentric distances 5-20 $R_\odot$ using the Indian Mars Orbiter Mission S-band radio signals. It is found that the turbulence power spectrum at smaller heliocentric distances ($< 10\ R_\odot$) displays flattening with a spectral index $\alpha_f \sim 0.2 - 0.4$, which corresponds to a solar wind acceleration region. At larger heliocentric distances ($> 10\ R_\odot$), the curve steepens, with a spectral index $\alpha_f \sim 0.6 - 0.8$, which is closer to the value 2/3 indicative of a developed Kolmogorov-type turbulence spectrum. The above analysis shows the important features of the transition in the solar wind turbulence regime, providing the indication of the location of the Alfvenic surface between 10-20 $R_\odot$. The experimental analysis presented here extends the results of various theoretical solar wind turbulence models [21] and contributes to the understanding of the process of turbulence energy transport by Alfvén waves, their non-linear transformation to magnetosonic waves, and dissipation leading to coronal heating and solar wind acceleration.

7. Acknowledgements

We acknowledge the efforts of the ground station team at Indian Deep Space Network, Bangalore India to track MOM radio signals at the D32 Antenna. Special thanks go to the MOM Mission team, UR Rao Satellite Centre, Bangalore for approve the tracking of MOM signals during solar conjunction, and to Shri CHK Bangararaju, and L. Srinivasan of ISRO Telemetry, Tracking and Command Network for conducting experiments. Thanks are also due to Himanshu Pandey and other staff at Indian Space Science Data Centre for their archiving and dissemination of data for further analysis.

8. References

1. Parker, E. N., “Dynamics of the Interplanetary Gas and Magnetic Fields.”, The Astrophysical Journal, vol. 128, p. 664, 1958. doi:10.1086/146579.

2. Hollweg J. V., “Transition region, corona, and solar wind in coronal holes”, 1986, J. Geophys. Res. , 91, 4111, doi : 10.1029/JA091iA04p04111

3. Jokipii J. R., “Turbulence and Scintillations in the Interplanetary Plasma”, 1973, ARA&A , 11, 1

4. Zirker J. B., “Coronal holes and high-speed wind streams”, 1977, Rev. Geophys.,15, 257, doi : 10.1029/RG015i003p00257

5. Geiss J., Gloeckler G., von Steiger R., “Origin of the Solar Wind From Composition Data”, 1995, Space Sci. Rev. , 72, 49

6. Coleman Paul J. J., “Turbulence, Viscosity, and Dissipation in the Solar-Wind Plasma”, 1968, ApJ , 153, 371

7. Cranmer S. R., van Ballegooijen A. A., Edgar R. J., “Self-consistent Coronal Heating and Solar Wind Acceleration from Anisotropic Magnetohydrodynamic Turbulence”, 2007, ApJS , 171, 520

8. Bruno R., Carbone V., “The Solar Wind as a Turbulence Laboratory” , 2013, Living Rev. Sol. Phys. , 10, 2

9. Adhikari, L.; Zank, G. P.; Zhao, L.-L., "Does Turbulence Turn off at the Alfvén Critical Surface?". *2019, The Astrophysical Journal.* **876** (1): 26, doi : 10.3847/1538-4357/ab141c

10. Chandran B. D. G., Perez J. C., 2019, “Reflection-driven magnetohydrodynamic turbulence in the solar atmosphere and solar wind”, J. Plasma Phys. , 85, 905850409

11. Verdini A., Velli M., “Alfven Waves and Turbulence in the Solar Atmosphere and Solar Wind”, 2007, ApJ , 662, 669

12. Wexler D. B., Hollweg J. V., Efimov A. I., Lukanina L. A., Coster A. J., Vierinen J., Jensen E. A., “Spacecraft Radio Frequency Fluctuations in the Solar Corona: MESSENGER Helios study” , 2019, ApJ , 871, 202

13. Efimov A. I., Chashei I. V., Bird M. K., Plettemeier D., Edenhofer P., Wohlmuth R., Samoznaev L. N., Lukanina L. A., “Turbulence in the Inner Solar Wind Determined from Frequency Fluctuations of the Downlink Signals from the ULYSSES and GALILEO Spacecraft” , 2005a, Adv. Space Res. , 36, 1448

14. Efimov A. I., Samoznaev L. N., Bird M. K., Chashei I. V., Plettemeier D., “Solar wind turbulence during the solar cycle deduced from Galileo coronal radio-sounding experiments” , 2008, Adv. Space Res. , 42, 117

15. Pätzold M., Hahn M., Tellmann S., Haeusler B., Bird M., Tyler G., Asmar S., Tsurutani B., “Coronal Density Structures and CMEs: Superior Solar Conjunctions of Mars Express, Venus Express, and Rosetta: 2004, 2006, and 2008” , 2012, Solar Phys. , 279

16. Richa N Jain, R K Choudhary, Anil Bhardwaj, Umang Parikh, Bijoy K Dai, M V Roopa, “A study on the solar coronal dynamics during the post-maxima phase of the solar cycle 24 using *S*-band radio signals from the Indian Mars Orbiter Mission”, *Monthly Notices of the Royal Astronomical Society*, 2022, 511, 2, 1750–1756, doi : 10.1093/mnras/stac056

17. Pätzold M. et al., 2004, MaRS: Mars Express Orbiter Radio Science. European Space Agency, (Special Publication) ESA SP

18. Armand N. A., Efimov A. I., Iakovlev O. I., “A model of the solar wind turbulence from radio occultation”, 1987, Astronomy & Astrophysics , 183, 135

19. Kasper J. C. et al., “Parker Solar Probe Enters the Magnetically Dominated Solar Corona”, 2021, Phys. Rev. Lett., 127, 255101

20. Woo R., Armstrong J. W.,”Spacecraft radio scattering observations of the power spectrum of electron density fluctuations in the solar wind”, 1979, J. Geophys. Res. (Space Phys.) , 84, 7288

21. Chashei I. V., Shishov V. I., “Solar Wind Turbulence in the Acceleration Region”, 1983, SvA, 27, 346